

Multispectral Analysis of Aerosols Over Oceans Using Principal Components

Thomas A. Jones and Sundar A. Christopher

Abstract—Applying principal component analysis (PCA) to one month of Moderate Resolution Imaging Spectroradiometer (MODIS) narrow-band short-wave radiance data and comparing with the Goddard Global Ozone Chemistry Aerosol Radiation Transport (GOCART) model simulations, we show that aerosol size and speciation information can be inferred from multispectral radiance information without having to use other parameters, such as a fine mode fraction (FMF), that are difficult to validate. PCA was applied to seven highly correlated MODIS solar channels (0.47, 0.55, 0.66, 0.86, 1.24, 1.64, and 2.12 μm) to extract noncorrelated pseudochannels, each with a unique interpretation. The first pseudochannel (PC1) can be interpreted as the mean radiance across the seven channels, which is directly proportional to the aerosol concentration. The second pseudochannel (PC2) is sensitive to the aerosol size since different aerosol types scatter and absorb differently across the seven MODIS short-wave channels. PC3 is inversely related to the aerosol optical thickness (AOT) and the FMF and appears most sensitive to changes in sulfate and maritime sea-salt concentrations. Results indicate that high values of PC1 are indicative of high dust aerosol concentrations comprising more than 40% of the total AOT, whereas high values of PC2 indicate anthropogenic aerosol concentrations (deduced from GOCART) in excess of 60%. Compared to simple 0.55- μm FMF thresholds, the PC channels are much more sensitive to dust aerosol concentrations and certain aspects of anthropogenic aerosols, with very low FMF values alone (< 0.2) being the best indicator of predominately sea-salt aerosol concentrations. Our results indicate that PCA could be used as an alternate method for inferring aerosol speciation information in future research over ocean and more complex land surfaces.

Index Terms—Aerosols, statistics.

35

I. INTRODUCTION

36 **W**ITH the advent of reliable satellite-derived data sets of 37 global aerosol properties, the climate effect of specific 38 aerosol types, particularly those anthropogenic in origin, has 39 become an important focus for research during the past 5 years 40 [1]. Moderate Resolution Imaging Spectroradiometer (MODIS) 41 provides radiance measurements in 36 channels from the ultra- 42 violet to the thermal part of the electromagnetic spectrum. The 43 MODIS aerosol algorithm over ocean uses the solar radiance at 44 seven channels (0.47, 0.55, 0.66, 0.86, 1.24, 1.64, and 2.12 μm)

[2] and then retrieves the aerosol optical thickness (AOT) using 45 a lookup table approach [2]. The multiwavelength capability 46 provides other retrievals such as the size, which is useful 47 for separating natural from anthropogenic aerosols [1]. The 48 spectral values of the AOT (τ) contain information about the 49 aerosol size, described by the Angstrom power law, i.e., 50

$$\tau = \beta \lambda^{-\alpha}. \quad (1)$$

Here, α is the wavelength exponent, β is the turbidity parameter, and λ is the wavelength in micrometers. The value of τ is dependent on the ratio of large to small aerosols, with large τ indicating the presence of high concentrations of small aerosols (e.g., smoke aerosols from biomass burning), and small τ indicating the presence of large aerosols, e.g., dust. Observational studies have made use of this size information such as small ($0.1 < r_e < 0.25 \mu\text{m}$) and coarse modes ($1.0 < r_e < 2.5 \mu\text{m}$) [sac1] AOT at 0.55 μm to discriminate between various aerosol types (e.g., [1]). The ratio of small to total AOT is known as the fine mode fraction (FMF) and has proven quite successful in separating predominately naturally occurring (coarse mode) from anthropogenic (small mode) aerosols [1], although it is a difficult parameter to validate [3]. In this method, MODIS AOT and FMF at 0.55 μm are used to separate the total AOT into various aerosol components using several thresholds [1]. AOT components are separated by first assuming that the maritime AOT is solely a linear function of near-surface wind speed over the ocean. The dust and anthropogenic components of the AOT are then solved using a mathematical relationship derived between the total AOT, the maritime AOT, the observed FMF, and the FMF thresholds. However, there are many assumptions required when separating the total AOT into various components such as the FMF thresholds themselves, and assuming that all small-mode aerosols are anthropogenic also leads to uncertainties in aerosol component radiative effects [3], [4].

The aerosol classification used by Kaufman *et al.* [1] and others generally uses aerosol information from only a single channel (usually at 0.55 μm), overlooking differences in the multispectral response for different aerosol types. Since each channel is highly correlated, we apply the principal component analysis (PCA) to extract the independent signals that are present in the seven-channel radiance data. Tanre *et al.* [5] used a similar PCA approach using theoretical radiance values for MODIS aerosol channels and observed that the AOT for small-mode aerosols decreases as a function of the wavelength much more quickly than for coarse-mode aerosols. Zubko *et al.* [6] extended this technique to other parameters, such as the single

Manuscript received November 27, 2007; revised February 23, 2008. This work was supported in part by the National Aeronautics and Space Administration (NASA) Radiation Sciences Program, in part by the NASA Interdisciplinary Sciences Program, in part by an Earth Observing System Grant, and in part by the Atmospheric Chemistry Modeling and Analysis Program.

The authors are with the Department of Atmospheric Science, The University of Alabama in Huntsville, Huntsville, AL 35805 USA (e-mail: tjones@nsstc.uah.edu; sundar@nsstc.uah.edu).

Color versions of one or more of the figures in this paper are available online at <http://ieeexplore.ieee.org>.

Digital Object Identifier 10.1109/TGRS.2008.920019

90 scattering albedo, the viewing angles, and the surface wind
 91 speed. Results from both efforts observed that two or three in-
 92 dependent pieces of information can be retrieved from MODIS
 93 multispectral radiance values through the PCA, and that these
 94 pieces of information account for more than 90% of the total
 95 variance present within the raw data. However, very little
 96 research has occurred that utilizes the multispectral characteris-
 97 tics of various aerosol species in aerosol classification using the
 98 PCA. In this study, the PCA is applied to the Terra MODIS
 99 radiance data at each channel, thereby producing a new set
 100 of independent channels, with each new channel sensitive to
 101 different aerosol characteristics. These data are then compared
 102 with the Goddard Global Ozone Chemistry Aerosol Radiation
 103 Transport (GOCART) modeled aerosol speciation during the
 104 same month and the Aerosol Robotic Network (AERONET)
 105 data from several sites that are known to have a single predom-
 106 inant aerosol species. The goal is to determine if multispectral
 107 PCA will provide information on aerosol species that cannot be
 108 observed using the $0.55\text{-}\mu\text{m}$ AOT and/or FMF alone.

109

II. DATA AND METHODS

110 Terra MODIS radiance values at $0.47, 0.55, 0.66, 0.86, 1.24,$
 111 1.64 , and $2.12\text{ }\mu\text{m}$ are obtained over the global oceans only
 112 from the MOD04, Collection 5 aerosol product [7], with a
 113 spatial resolution of 10 km^2 at nadir. We use the raw radiance
 114 values as inputs to the PCA rather than the retrieved AOT
 115 values at each wavelength since AOT retrievals are already a
 116 function of all seven radiance channels. For increasing aerosol
 117 concentrations, for scattering types of aerosols, larger amounts
 118 of short-wave radiation are scattered back to the satellite, re-
 119 sulting in a higher observed top of atmosphere radiance values.
 120 The AOT values over the ocean are retrieved from MODIS
 121 radiance values using a combination of four small-mode and
 122 five coarse-mode aerosol models with the relative amounts of
 123 small-mode to coarse-mode aerosols adjusted until a solution
 124 is found, which minimizes the error across the seven radiance
 125 values [2]. As a result, the reported AOT values at a certain
 126 wavelength are dependent on the radiance values from other
 127 channels. Using the retrieved AOT would induce uncertainties
 128 and biases that are present in the MODIS aerosol models into
 129 the research presented here. Thus, we chose to use the mea-
 130 sured MODIS cloud-free radiance values as inputs to the PCA
 131 rather than any derived products. MODIS data are collected for
 132 August 2004 due to the variety of differing aerosol types around
 133 the globe during this month. MODIS AOT and FMF from the
 134 MOD04 level 2 product from the Terra satellite along with the
 135 AERONET AOT values are used to help interpret the PCA
 136 components. The AERONET is a network of well-calibrated
 137 ground-based sun photometers that provide spectral AOT and
 138 other aerosol properties from hundreds of locations around
 139 the world [8]. We use the data for August 22, August 16,
 140 and August 10, 2004, from AERONET sites Capo Verde,
 141 Gosan (Korea), and Ascension Island, which are compared
 142 and colocated with the MODIS AOT data for that day. Data
 143 from these days were selected based on times when both good
 144 quality AERONET and MODIS data exist. For a particular
 145 day, MODIS AOT data within $\pm 1^\circ$ of the AERONET site

were averaged and compared to the AERONET observations. 146
 Each site location represents where the primary aerosol source 147
 (other than maritime sea salt) is known *a priori* from GOCART, 148
 including dust, fossil fuel combustion, and biomass burning, 149
 respectively. 150

The satellite-retrieved AOT and FMF are compared with the 151
 aerosol species simulations produced by the GOCART model 152
 [9]. GOCART simulates the transport of aerosols and their 153
 type over a global domain on a monthly averaged timescale. 154
 GOCART uses global emissions of aerosols and assimilated 155
 meteorological fields to separately calculate the mass loading 156
 of each aerosol species, which are then converted to the AOT 157
 using mass extinction coefficients. Aerosols are categorized as 158
 black carbon (BC), organic carbon (OC), sulfate (SU), dust 159
 (DU), and sea salt (SS). Organic carbon and sulfate are also 160
 split into anthropogenic and naturally occurring components, 161
 the latter generally from dimethyl sulfide (DMS). Monthly 162
 averaged data for August 2004 were acquired for an ocean only, 163
 global domain and were interpolated to a $2^\circ \times 2^\circ$ grid. 164

The statistical technique of the PCA enables the reduction 165
 of multiple and highly correlated data attributes into a fewer 166
 number of independent variables, each with a unique physical 167
 interpretation [10], [11]. The initial step in the PCA is the 168
 calculation of a correlation matrix between each of the input 169
 channels, which are the radiance values at all seven MODIS 170
 channels. Once the correlation matrix is computed, eigenvalues 171
 and vectors are calculated from the correlation matrix to deter- 172
 mine the weighting coefficients, which are then applied to the 173
 radiance data to produce the new independent pseudochannels 174
 (or PC channels). Each PC channel is ordered in such a way 175
 that the first channel (PC1) accounts for the greatest variance 176
 in the raw data, with the next (PC2) accounting for the next 177
 highest amount of variance, and so on. For this paper, the total 178
 number of pseudochannels created is equal to the number of 179
 input channels, which is seven. For illustration purposes, PC 180
 values are normalized to a $0\text{--}1.0$ scale and averaged to a $2^\circ \times 2^\circ$ 181
 resolution grid to correspond with the monthly averaged GO- 182
 CART data resolution. To visualize the sensitivity of the PC 183
 channels to aerosol properties, we compare GOCART and 184
 MODIS data as a function of the PC value. PC values are binned 185
 at 0.05 intervals, and, for each bin, the ratio of the GOCART 186
 component AOT to the total AOT is calculated for grid cells 187
 within a particular PC bin. To compare the effectiveness of the 188
 PC classification with the $0.55\text{-}\mu\text{m}$ FMF classification, a similar 189
 procedure is used but using a 0.05 FMF interval bin. 190

III. RESULTS

A. PC Weightings

As expected, solar radiance from each of the seven MODIS 193
 aerosol channels is highly correlated, although the correlation 194
 does decrease to < 0.5 when comparing $0.47\text{-}2.13\text{-}\mu\text{m}$ 195
 radiance values. Analysis of the eigenvalues associated with 196
 each PC channel indicates that 78.4% of the variance is ex- 197
 plained by PC1, 19.7% by PC2, and 1.4% by PC3, with PC1– 198
 PC3 accounting for $\sim 99\%$ of the total variance, similar to that 199
 expected in [5] and [6]. The amount explained by PC4–PC7 200
 combined is less than 1%, with no consistent patterns observed 201

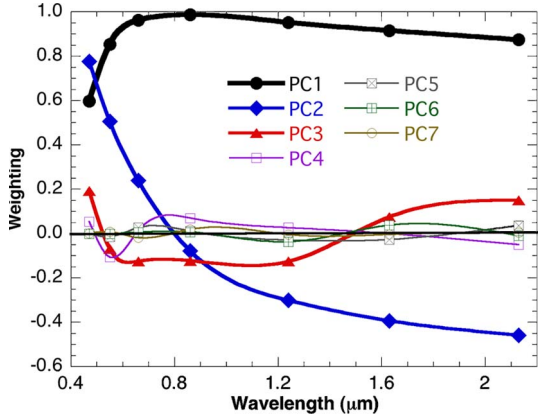


Fig. 1. Weighting coefficients derived from the PCA for PC channels 1–7. Magnitudes indicate the relative importance of each original channel to the resulting PC channel. Note that weightings for PC4–PC7 are very small compared to those for PC1–PC3.

202 in the weighting coefficients. Thus, we are confident that nearly
203 all of the physical signals present in the seven-channel radiance
204 data are taken into account by the first three pseudochannels
205 (PC1–PC3). These values are only representative of the one-
206 month data set examined here; however, they remain rel-
207 atively constant compared to the remaining 11 months of
208 2004: $74\% < \text{PC1} < 84\%$; $15\% < \text{PC2} < 24\%$; $1\% < \text{PC3} <$
209 2%. The physical interpretation of PC1–PC3 also remains the
210 same despite the presence of differing aerosol concentrations
211 and types from month to month.

212 Raw weighting coefficients as a function of the MODIS
213 wavelength are plotted in Fig. 1. The coefficients indicate
214 the relative contribution of each original channel to the new
215 pseudochannel. PC1 has, by far, the highest weightings com-
216 pared to PC2 and PC3. Physically, PC1 represents a weighted
217 mean or “multispectral” radiance value that is directly propor-
218 tional to the aerosol concentration, with low values of PC1
219 corresponding to low values of the AOT (for all original wave-
220 lengths), whereas high PC1 values correspond to high values
221 of the AOT at $0.55\text{ }\mu\text{m}$ (Fig. 2). The correlation between PC1
222 and the AOT at $0.55\text{ }\mu\text{m}$ is high ($r = 0.89$) and is generally
223 linear for $\text{AOT} < 1.0$. This linear relationship is similar to that
224 observed between the AOT and the broadband short-wave flux,
225 which itself is highly correlated with the MODIS narrow-band
226 short-wave observations [12].

227 A more interesting relationship exists in PC2. Weighting
228 coefficients for PC2 decrease as the MODIS wavelength in-
229 creases, and range from 0.78 at $0.47\text{ }\mu\text{m}$ (blue) to -0.46 at
230 $2.12\text{ }\mu\text{m}$ (near infrared) with a weighting of near zero at
231 $0.86\text{ }\mu\text{m}$ (Fig. 1). Due to its small weighting coefficient, the
232 radiance at $0.86\text{ }\mu\text{m}$ contributes very little to PC2 values.
233 These weightings indicate that PC2 is the most sensitive to
234 the difference between blue and red radiance values, which
235 would be greatest for aerosols that scatter more radiation in
236 the blue portion of the spectrum and for aerosols that scatter
237 proportionally less radiation in the near-infrared portion of the
238 spectrum. Compared to PC1, PC2 is only weakly correlated
239 with the AOT at $0.55\text{ }\mu\text{m}$, with a correlation coefficient of
240 only -0.11 (Fig. 2). However, the correlation between PC2 and
241 the FMF at $0.55\text{ }\mu\text{m}$ is much higher, i.e., 0.54, indicating the

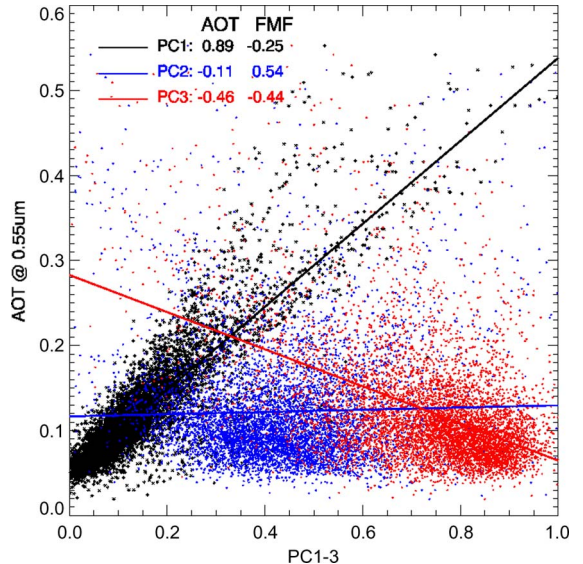


Fig. 2. Scatterplot of monthly averaged MODIS AOT at $0.55\text{ }\mu\text{m}$ as a function of normalized PC1, PC2, and PC3 values. Best-fit lines along with linear correlation coefficients between PC values and MODIS AOT and FMF are also given.

dependence on the aerosol size. A similar result was observed
242 by Tanre *et al.* [5], who also noted that this relationship was
243 the most important for small-sized aerosols ($r_e < 0.3\text{ }\mu\text{m}$).
244 Previous research has observed that anthropogenic aerosols,
245 which are primarily small mode in nature, often have higher
246 blue versus near-infrared radiance values (e.g., [13]). Thus,
247 PC2 could be useful for separating naturally occurring from
248 anthropogenic aerosol regions since it is correlated with aerosol
249 size properties.

The interpretation of PC3 is not as clear as those of PC1 and
251 PC2. Weighting coefficient values are quite small ($< \pm 0.2$) and
252 are positive for MODIS $0.47\text{-, }1.24\text{-, and }2.12\text{-}\mu\text{m}$ channels,
253 but negative for the remaining four channels. PC3 shows a
254 modest inverse correlation with the AOT and the FMF at
255 $0.55\text{ }\mu\text{m}$ ($r = -0.46, -0.44$; Fig. 2). Interestingly, the shape
256 of the weighting coefficient curve mirrors that observed for
257 PC1 to some extent, which is consistent with the reversed sign
258 of the AOT correlation. Although PC3 only explains a small
259 proportion of the total variance, the significance of the AOT
260 and FMF correlations suggests that it is indeed an actual signal
261 and not random noise. The correlation between PC4–PC7 and
262 the AOT or the FMF at $0.55\text{ }\mu\text{m}$ never exceeds 0.15, making
263 the physical interpretation of these channels difficult if such an
264 interpretation exists at all.

Additional evidence for the physical interpretation of PC
266 channels can be found when comparing multispectral MODIS
267 and AERONET AOT values for locations where the predomi-
268 nant aerosol source is known. The locations selected are Capo
269 Verde, Gosan (Korea), and Ascension Island, whose aerosol
270 concentrations are largely from dust, fossil fuel combustion,
271 and biomass burning, respectively. Fig. 3 shows MODIS and
272 AERONET AOT values as a function of the wavelength. For
273 all three locations, MODIS AOT decreases as a function of the
274 wavelength. However, the decrease is much more significant
275 (compared to the average AOT across all channels) for Gosan
276

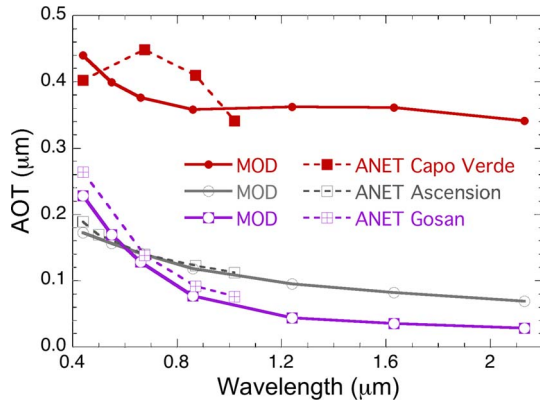


Fig. 3. MODIS (MOD) and AERONET (ANET) AOT between 0.4 and 2.2 μm for three sites, Capo Verde, Gosan (Korea), and Ascension Island, each representing significant dust, industrial pollution, and biomass burning aerosol concentrations, respectively. Note the similarities between Gosan and Ascension Island AOT and PC2 weighting coefficients.

277 (Korea) and Ascension Island locations, where small-mode
278 aerosol concentrations are significant [14]. AERONET AOT for
279 these two sites closely follows that of MODIS AOT, although
280 some differences were observed at Capo Verde. Levy *et al.* [15]
281 noted the differences in the multispectral response to dust
282 aerosols between MODIS and AERONET measurements. Their
283 differences are different than those observed here; however,
284 we use Collection 5 data, which have improved coarse-mode
285 aerosol models not used by Levy *et al.* [15]. However, the
286 spectral response for small-mode aerosols for both MODIS
287 and AERONET AOT remains clearly significant. Also, the de-
288 creasing AOT as a function of increasing wavelength for these
289 aerosols corresponds quite well with the weighting coefficients
290 for PC2, indicating that it is indeed sensitive to the aerosol size
291 (Figs. 1 and 3).

292 The usefulness of this multispectral approach toward aerosol
293 classification is evident when creating a three-band overlay
294 using normalized PC1, PC2, and PC3 values (Fig. 4). Here,
295 high values of PC1, PC2, and PC3 are denoted by red, green,
296 and blue colors, respectively. Brightness increases as the values
297 for PC1–PC3 become larger. It is immediately clear that aerosol
298 speciation information is evident when utilizing the first three
299 PC channels. Regions normally associated with dust (eastern
300 North Atlantic and western Arabian Sea) in August appear
301 as pink and red, which indicates that high values of PC1
302 correspond to high concentrations of dust aerosols compared
303 to other aerosol types. Yellow-green regions are present in the
304 South Atlantic Ocean off west of Africa and, to a lesser degree,
305 in Indonesia and east of China. Anthropogenic aerosols, in
306 the form of sulfates and organic carbon, are the predominant
307 aerosol types in these regions. The signal is most evident in the
308 South Atlantic, where large amounts of aerosols from biomass
309 burning are transported over the ocean. Since the AOT is high
310 and the FMF is low, PC1 and PC2 values are high, resulting
311 in the yellow color observed. Light blues and greens are also
312 evident off the east coasts of the U.S. and northern Europe.
313 Compared to the dust and biomass burning regions, the total
314 AOT is low (low red values), but the anthropogenic (particularly
315 sulfate) proportion of aerosols is high resulting in the greenish
316 appearance. Regions over the open oceans appear blue, corre-

sponding to high values of PC3. Here, aerosol concentrations 317 are generally low (low PC1) and consist of maritime sea salt 318 and DMS (low PC2). In the Southern Hemisphere south of 319 35 °S, somewhat higher values of PC1 were observed, possibly 320 resulting from larger sea-salt concentrations due to high wind 321 speeds or cloud contamination [16].

B. PC Values Compared to GOCART Aerosol Components

To determine the sensitivity of each PC channel to specific 324 aerosol properties, PC1–PC3 values are compared to monthly 325 averaged GOCART model-generated aerosol speciation over 326 the global oceans for August 2004. Fig. 5(a)–(c) shows av- 327 erage MODIS AOT and FMF at 0.55 μm as a function of 328 normalized PC1–PC3, binned at 0.05 intervals. Also plotted 329 is the percentage of the total GOCART AOT at 0.55 μm 330 accounted for by one of the six aerosol species, including 331 sea salt (SS), dust (DU), black carbon (BC), anthropogenic 332 organic carbon (OC), anthropogenic sulfate (SU), and naturally 333 occurring sulfate (NSU). MODIS AOT increases from 0.08 to 334 0.60 as PC1 increases from 0 to 1.0, as should be the case given 335 the high correlation between PC1 and short-wave radiance at 336 most channels [Fig. 5(a)]. The FMF remains roughly constant 337 at ~ 0.5 when $0.2 < \text{PC1} < 0.8$, although it does vary at the low 338 and high extremes of PC1. Comparing PC1 values to GOCART 339 aerosol speciation shows several interesting features. The nat- 340 urally occurring portion of organic carbon was always small, 341 never being greater than 3%, and, thus, was not plotted. DMS 342 accounts for up to 15% when $\text{PC1} < 0.2$, but less than 10% 343 thereafter. The anthropogenic sulfate concentration remains 344 between 20% and 25% for all PC1 bins. However, the dust 345 aerosol concentration does substantially change as a function of 346 PC1, ranging from 15% to 50% at the expense of sea salt and 347 natural and organic sulfate concentrations. Since low aerosol 348 concentrations often occur over the open oceans, the high sea- 349 salt concentration at low PC1 values should exist, although, 350 even for low PC1 values, the total sea-salt portion of the AOT 351 does not exceed 30%. The low values of PC1 ($\text{PC} < 0.2$) 352 correspond to relatively pristine ocean conditions, where sea 353 salt and DMS are the primary aerosol species, whereas the high 354 values of PC1 correspond to high dust aerosol concentrations. 355 PC1 values show little sensitivity to black and organic carbon 356 concentrations.

Aerosol properties also substantially change as a function of 358 PC2 values [Fig. 5(b)]. Unlike PC1, PC2 is sensitive to changes 359 in the aerosol size, evidenced by the increasing FMF values 360 as a function of PC2. Moreover, unlike PC1, PC2 is not very 361 sensitive to the total aerosol concentration with a very little 362 change in MODIS AOT when $0.2 < \text{PC2} < 0.8$, whereas the 363 FMF increases from 0.3 to 0.7 over that same range. Corre- 364 sponding to this increase in the FMF, anthropogenic organic 365 carbon and sulfate, which are both generally considered small- 366 mode aerosols, substantially increase accounting for over 50% 367 of the total AOT when $\text{PC2} > 0.8$. The portion of the AOT 368 due to black carbon also slightly increases, but remains below 369 10%. The dust aerosol concentration generally represents less 370 than 20% of the total AOT for all PC2 bins, with no apparent 371 trends. The sea-salt concentration rapidly decreases with values 372

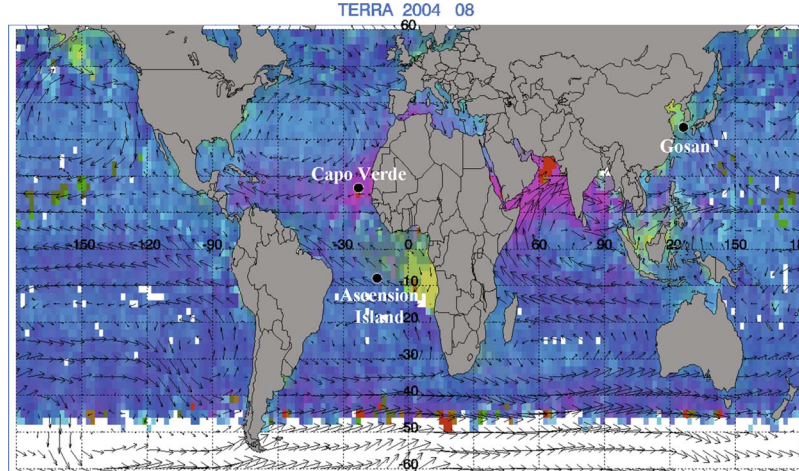


Fig. 4. Three-band overlay of normalized (red) PC1, (green) PC2, and (blue) PC3 values for August 2004. Locations of AERONET sites (Capo Verde, Gosan, and Ascension Island) are represented by black circles.

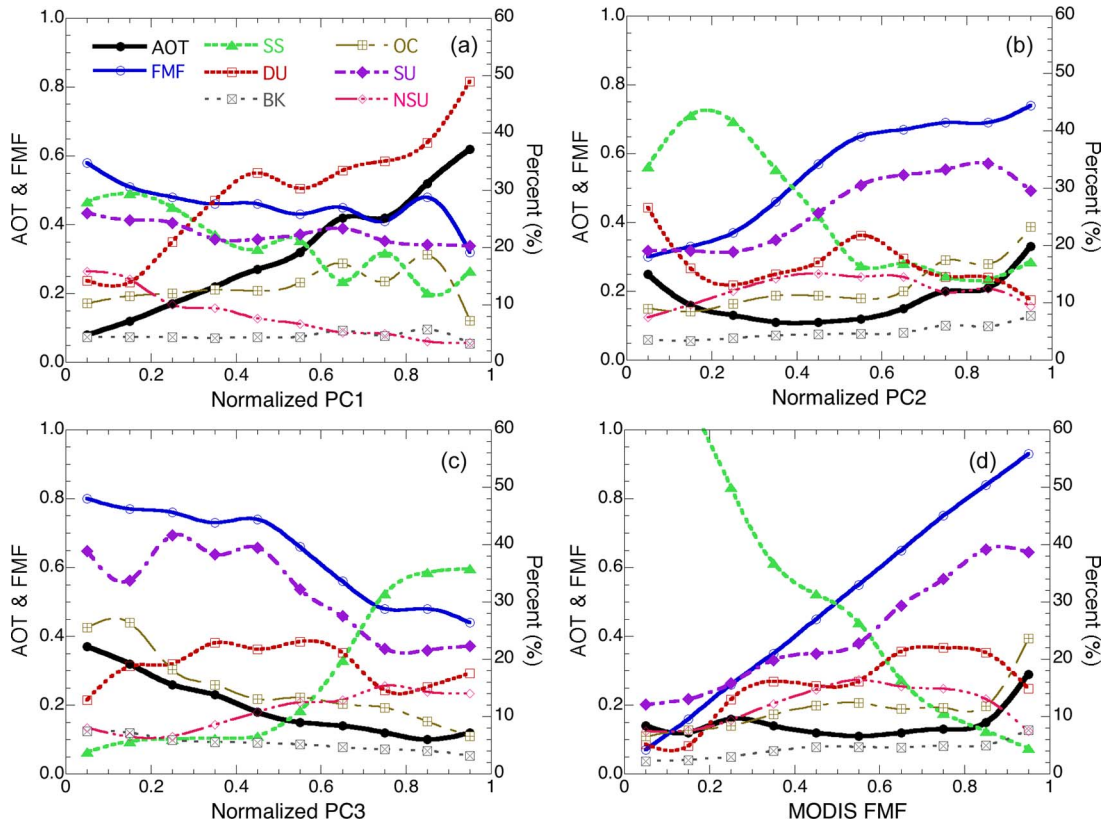


Fig. 5. MODIS AOT, FMF, and GOCART-modeled contribution to the total AOT for six major aerosol species (sea salt, dust, black carbon, anthropogenic organic carbon, anthropogenic sulfate, and naturally occurring sulfate) as a function of a normalized PC value for (a) PC1, (b) PC2, (c) PC3, and (d) FMF at $0.55 \mu\text{m}$.

373 exceeding 40% for $\text{PC2} < 0.3$, but decreasing to less than 20%
 374 thereafter. These results indicate that PC2 are the sensitive
 375 aerosols produced from anthropogenic sources, particularly
 376 biomass burning occurring off the African coast (Fig. 4). For
 377 PC2 greater than 0.8, the total anthropogenic component of the
 378 AOT ($\text{BC} + \text{OC} + \text{SU}$) represents over 60% of the total AOT
 379 modeled by GOCART, whereas the combined dust and sea-salt
 380 contribution represents less than 30% of the total AOT.
 381 The third PC channel, i.e., PC3, is an interesting case.
 382 Although it only accounts for 1.4% of the total variance,

the weighting coefficients show a distinct pattern, somewhat 383 mirroring the shape of PC1 weightings (Fig. 1). Fig. 2 suggests 384 that PC3 is equally sensitive to the aerosol concentration as well 385 as the aerosol size parameters. Comparing PC3 values against 386 GOCART-modeled aerosol species also reveals that this PC is 387 also useful in the separation of aerosol species. Unlike PC1 388 and PC2, sea-salt and DMS contributions increase for larger 389 PC3 values that when combined, become $> 50\%$ for $\text{PC3} > 0.8$ [Fig. 5(c)]. A corresponding decrease in anthropogenic 391 organic carbon and sulfate is also observed, with little overall 392

393 sensitivity to the dust aerosol concentration. The decrease in
 394 anthropogenic aerosol concentrations corresponds with similar
 395 decreases in MODIS FMF and AOT values [Figs. 2 and 5(c)].
 396 Thus, PC3 can be said to be inversely proportional to the aerosol
 397 size and the total aerosol concentration, PC1 is primarily sen-
 398 sitive to the total aerosol concentration, and PC2 is primarily
 399 sensitive to the aerosol size but not to the concentration, consis-
 400 tent with Fig. 2. PC3 is statistically independent to PC2; thus,
 401 the multispectral radiance values are providing two independent
 402 sources of aerosol size and concentration information.

403 The exact physical mechanism behind PC3 remains unclear;
 404 however, spatial plots of PC3 alone (not shown) clearly show
 405 high values in maritime regions, whereas the plots show very
 406 low values in regions associated with aerosols transported
 407 from biomass burning sources. One possible hypothesis is the
 408 sensitivity of the 0.47- μm channels toward ocean reflectance,
 409 which also happens to have a positive weighting coefficient in
 410 PC3 (Fig. 1). Thus, it is possible that the high values of PC3
 411 correspond to low AOT concentrations when the ocean re-
 412 flectance signal is the strongest. Similarly, PC3 is minimized
 413 when the AOT is high, masking the ocean reflectance signal
 414 from the satellite. However, this hypothesis still does not ex-
 415 plain the positive coefficients present at 1.63- and 2.12- μm
 416 wavelengths. This remains a question for future research to
 417 answer. For higher order PC channels (PC4–PC7), there ap-
 418 pears to be very little sensitivity to aerosol properties. With the
 419 exception of weak sensitivity to the natural sulfate concentra-
 420 tion for PC5, GOCART-modeled aerosol properties showed no
 421 consistent trends as a function of PC values (not shown). For the
 422 purposes of aerosol classification, these channels provide little
 423 in the way of useful information.

424 C. MODIS FMF Values Compared to GOCART 425 Aerosol Components

426 To determine if principal components are indeed useful, we
 427 perform the same analysis as above, but for MODIS FMF
 428 values [Fig. 5(d)]. It is quite evident that FMF values are an
 429 excellent way to distinguish among sea-salt and anthropogenic
 430 sulfate and organic carbon aerosols. When $\text{FMF} < 0.2$, the
 431 proportion of the AOT from sea salt exceeds 60%, whereas
 432 the anthropogenic aerosol contribution approaches 60% for
 433 $\text{FMF} > 0.8$, with most of the anthropogenic contribution being
 434 from sulfate. However, the FMF alone is not very sensitive
 435 to the dust aerosol concentration. There is an increase in the
 436 dust proportion from $\sim 10\%$ at a low FMF to $\sim 20\%$ at a high
 437 FMF, which actually contradicts the expectations. Generally,
 438 dust aerosols have larger particle sizes than the anthropogenic
 439 components: thus, one would expect the dust concentrations to
 440 be greatest somewhere around $\text{FMF} \approx 0.5$ [1]. At least for the
 441 time period used here, dust aerosols are sufficiently mixed with
 442 other aerosol types for their signal to be not apparent in MODIS
 443 FMF observations alone. However, performing the PCA on
 444 the raw MODIS radiance values produces a pseudochannel
 445 (PC1) that is sensitive to the dust aerosol concentration to
 446 a much higher degree. Since PC1 is highly correlated with
 447 the total AOT, one might expect that the total AOT is also
 448 sensitive to the dust aerosol concentration; however, this, again,

449 was not observed here (not shown). Rather, we believe that
 450 it is the multispectral response of dust aerosols compared to
 451 anthropogenic types that produces this signal. These differences
 452 are apparent in Fig. 1, with the AERONET AOT dust spectral
 453 dependence being of different shape than the other two aerosol
 454 types. This shape is quite similar to the weighting value curve
 455 plotted in Fig. 1; thus, high concentrations of dust are most
 456 likely to result in high values of PC1. 456

D. Application of Weighting to Independent Data

457

To access the applicability of the weighting coefficients to 458 independent data, we apply the coefficients derived from the 459 Terra data above to the MODIS data from the Aqua satellite 460 acquired for the same month (August 2004). Aside from the 461 Aqua overpass being 3–4 h after Terra, everything else related 462 to the retrievals of aerosol radiance should be the same. If we 463 assume that aerosol properties do not significantly change in 464 this short time, applying the Terra weighting coefficients to 465 Aqua data should produce good results. The Terra weighting 466 coefficients are applied to the Aqua MODIS radiance values 467 producing one set of PC data, which are compared with another 468 set of PC data produced from the Aqua radiance values using 469 the weighing coefficients derived from the Aqua data itself. The 470 resulting correlation between these data is greater than 0.99 471 for PC1–PC3. For higher order PC channels, the correlation 472 substantially decreases, as random noise becomes a more sig- 473 nificant factor. 474

IV. CONCLUSION

475

We have shown that multispectral AOT data from the MODIS 476 satellite in conjunction with GOCART can be used to extract 477 important aerosol type information without the use of small- 478 mode AOT values. The PCA condenses seven highly correlated 479 radiance channels into a smaller number of independent PC 480 channels, each with its own physical interpretation. Using the 481 monthly averaged GOCART data as a guide, it becomes appar- 482 ent that different PC channels are sensitive to various aerosol 483 species and mixtures thereof. We show that PC1 and PC3 can 484 distinguish between pristine (sea salt and DMS) and heavy 485 dust aerosol concentrations, whereas PC2 is very sensitive to 486 anthropogenic aerosol concentrations, with high PC2 values 487 corresponding to a 60% or greater anthropogenic component 488 to the total AOT. PC data, particularly PC1, are much more 489 sensitive to the dust aerosol concentration compared to the use 490 of simple FMF thresholds. Since dust aerosol concentrations 491 are often the most difficult type to extract on an objective basis, 492 perhaps future works could take advantage of the approach 493 examined here. It is likely that the use of higher spatial and tem- 494 poral resolution aerosol speciation modeling allows for even 495 better multispectral aerosol characteristics to be drawn. With 496 higher resolution GOCART data, higher order PC channels may 497 also be able to provide additional information into the observed 498 aerosol properties. Given the problems noted with satellite- 499 derived aerosol parameters over land, the use of multispectral 500 information provides another, possibly more effective, avenue 501 for aerosol classification over land. Future research will analyze 502

503 this possibility using larger data sets encompassing multiple
504 years of observations.

505

ACKNOWLEDGMENT

506 The Clouds and the Earth's Radiant Energy System (CERES)
507 Single Scanner Footprint data, which contain the merged
508 MODIS and CERES and the Measurements of Pollution in
509 the Troposphere data were obtained through the NASA Lan-
510 gley Distributed Active Archive Systems. The MODIS daily
511 products were obtained from the Goddard Distributed Active
512 Archive Systems. The authors would like to thank Dr. M. Chin
513 for providing the GOCART results.

514

REFERENCES

- 515 [1] Y. J. Kaufman, O. Boucher, D. Tanre, M. Chin, L. A. Remer,
516 and T. Takemura, "Aerosol anthropogenic component estimated from
517 satellite data," *Geophys. Res. Lett.*, vol. 32, no. 17, L17 804, 2005.
518 DOI:10.1029/2005GL023125.
- 519 [2] L. A. Remer, Y. J. Kaufman, D. Tanré, S. Mattoo, D. A. Chu,
520 J. V. Martins, R.-R. Li, C. Ichoku, R. C. Levy, R. G. Kleidman, T. F. Eck,
521 E. Vermote, and B. N. Holben, "The MODIS aerosol algorithm, products,
522 and validation," *J. Atmos. Sci.*, vol. 62, no. 4, pp. 947–973, Apr. 2005.
- 523 [3] T. L. Anderson *et al.*, "An 'A-Train' strategy for quantifying direct climate
524 forcing by anthropogenic aerosols," *Bull. Amer. Meteorol. Soc.*, vol. 86,
525 no. 12, pp. 1795–1809, Dec. 2005.
- 526 [4] T. A. Jones and S. A. Christopher, "Statistical variability of top of at-
527 mosphere cloud-free shortwave aerosol radiative effect," *Atmos. Chem.
528 Phys. Discuss.*, vol. 7, pp. 2937–2948, 2007.
- 529 [5] D. Tanre, M. Herman, and Y. J. Kaufman, "Information on aerosol size
530 distribution contained in solar reflected spectral radiances," *J. Geophys.
531 Res.*, vol. 101, no. D14, pp. 19 043–19 060, 1996.
- 532 [6] V. Zubko, Y. J. Kaufman, R. I. Burg, and J. V. Martins, "Principal com-
533 ponent analysis of remote sensing of aerosols over oceans," *IEEE Trans.
534 Geosci. Remote Sens.*, vol. 45, no. 3, pp. 730–745, Mar. 2007.
- 535 [7] L. A. Remer, D. Tanre, and Y. Kaufman, *Algorithm for Remote Sensing of
536 Tropospheric Aerosol From MODIS: Collection 5*, 2006.
- 537 [8] B. N. Holben *et al.*, "AERONET—A federated instrument network and
538 data archive for aerosol characterization," *Remote Sens. Environ.*, vol. 66,
539 no. 1, pp. 1–16, Oct. 1998.
- 540 [9] M. Chin *et al.*, "Aerosol distributions and radiative properties simulated in
541 the GOCART model and comparisons with observations," *J. Atmos. Sci.*,
542 vol. 59, pp. 461–483, 2002.
- 543 [10] T. A. Jones, K. M. McGrath, and J. T. Snow, "Association between
544 NSSL mesocyclone detection algorithm-detected vortices and tornadoes,"
545 *Weather Forecast.*, vol. 19, no. 5, pp. 872–890, Oct. 2004.
- 546 [11] D. S. Wilks, *Statistical Methods in the Atmospheric Sciences*. San Diego,
547 CA: Academic, 2006.
- 548 [12] N. G. Loeb and N. Manalo-Smith, "Top-of-atmosphere direct radiative
549 effect of aerosols over global oceans from merged CERES and MODIS
550 observations," *J. Climate*, vol. 18, no. 17, pp. 3506–3526, Sep. 2005.

- [13] T. F. Eck *et al.*, "Wavelength dependence of the optical depth of biomass
551 burning, urban, and desert dust aerosols," *J. Geophys. Res.*, vol. 104, 552
no. D24, pp. 31 333–31 349, 1999.
553
- [14] A. Smirnov, B. N. Holben, Y. J. Kaufman, O. Dubovik, T. F. Eck,
554 I. Slutsker, C. Pietras, and R. N. Halthore, "Optical properties of at-
555 mospheric aerosol in maritime environments," *J. Atmos. Sci.*, vol. 59, 556
no. 3, pp. 501–523, Feb. 2002.
557
- [15] R. C. Levy, L. A. Remer, S. Mattoo, E. F. Vermote, and Y. J. Kaufman,
558 "Second-generation operational algorithm: Retrieval of aerosol properties
559 over land from inversion of moderate resolution imaging spectroradiome-
560 ter spectral reflectance," *J. Geophys. Res.*, vol. 112, no. D13, D13 211, 561
Jul. 2007. DOI: 10.1029/2006JD007811.
562
- [16] J. Zhang, J. S. Reid, and B. N. Holben, "An analysis of potential
563 cloud artifacts in MODIS over ocean aerosol optical thickness prod-
564 ucts," *Geophys. Res. Lett.*, vol. 32, no. 15, L15 803, Aug. 2005. DOI:
565 10.1029/2005GL023254.
566



Thomas A. Jones received the B.S. and M.S. 567 degrees in meteorology from the University of 568 Oklahoma, Norman, in 2000 and 2002, respectively, 569 while focusing on the development of regional thun- 570 derstorm climatologies, and the Ph.D. degree from 571 The University of Alabama in Huntsville, Huntsville, 572 in 2006 while specializing in improving hurricane in- 573 tensity change forecasts using satellite-derived pas- 574 sive microwave imagery. 575

Since May 2006, he has been a Research Scientist 576 with The University of Alabama in Huntsville. He 577 has a wide range of research interests within the atmospheric sciences commu- 578 nity. He is currently researching the effect of aerosols, and their subspecies, on 579 short-wave and long-wave radiative effects using MODIS and CERES data. He 580 is extending this research to include the effects of meteorological conditions on 581 aerosols and the aerosol's effect to clouds. 582



Sundar A. Christopher received the M.S. degree 583 in meteorology from the South Dakota School of 584 Mines and Technology, Rapid City, in 1989, the M.S. 585 degree in industrial/organizational psychology from 586 The University of Alabama in Huntsville (UAH), 587 Huntsville, in 2002, and the Ph.D. degree in at- 588 mospheric sciences from the Colorado State Univer- 589 sity, Fort Collins, in 1995. 590

He is currently a Professor with the Department of 591 Atmospheric Sciences and the Associate Director of 592 the Earth System Science Center, both at UAH. His 593 research interests include satellite remote sensing of clouds and aerosols and 594 their impact on air quality and global and regional climate. 595

Multispectral Analysis of Aerosols Over Oceans Using Principal Components

Thomas A. Jones and Sundar A. Christopher

Abstract—Applying principal component analysis (PCA) to one month of Moderate Resolution Imaging Spectroradiometer (MODIS) narrow-band short-wave radiance data and comparing with the Goddard Global Ozone Chemistry Aerosol Radiation Transport (GOCART) model simulations, we show that aerosol size and speciation information can be inferred from multispectral radiance information without having to use other parameters, such as a fine mode fraction (FMF), that are difficult to validate. PCA was applied to seven highly correlated MODIS solar channels (0.47, 0.55, 0.66, 0.86, 1.24, 1.64, and 2.12 μm) to extract noncorrelated pseudochannels, each with a unique interpretation. The first pseudochannel (PC1) can be interpreted as the mean radiance across the seven channels, which is directly proportional to the aerosol concentration. The second pseudochannel (PC2) is sensitive to the aerosol size since different aerosol types scatter and absorb differently across the seven MODIS short-wave channels. PC3 is inversely related to the aerosol optical thickness (AOT) and the FMF and appears most sensitive to changes in sulfate and maritime sea-salt concentrations. Results indicate that high values of PC1 are indicative of high dust aerosol concentrations comprising more than 40% of the total AOT, whereas high values of PC2 indicate anthropogenic aerosol concentrations (deduced from GOCART) in excess of 60%. Compared to simple 0.55- μm FMF thresholds, the PC channels are much more sensitive to dust aerosol concentrations and certain aspects of anthropogenic aerosols, with very low FMF values alone (< 0.2) being the best indicator of predominately sea-salt aerosol concentrations. Our results indicate that PCA could be used as an alternate method for inferring aerosol speciation information in future research over ocean and more complex land surfaces.

Index Terms—Aerosols, statistics.

35

I. INTRODUCTION

36 **W**ITH the advent of reliable satellite-derived data sets of 37 global aerosol properties, the climate effect of specific 38 aerosol types, particularly those anthropogenic in origin, has 39 become an important focus for research during the past 5 years 40 [1]. Moderate Resolution Imaging Spectroradiometer (MODIS) 41 provides radiance measurements in 36 channels from the ultra- 42 violet to the thermal part of the electromagnetic spectrum. The 43 MODIS aerosol algorithm over ocean uses the solar radiance at 44 seven channels (0.47, 0.55, 0.66, 0.86, 1.24, 1.64, and 2.12 μm)

[2] and then retrieves the aerosol optical thickness (AOT) using 45 a lookup table approach [2]. The multiwavelength capability 46 provides other retrievals such as the size, which is useful 47 for separating natural from anthropogenic aerosols [1]. The 48 spectral values of the AOT (τ) contain information about the 49 aerosol size, described by the Angstrom power law, i.e., 50

$$\tau = \beta \lambda^{-\alpha}. \quad (1)$$

Here, α is the wavelength exponent, β is the turbidity parameter, and λ is the wavelength in micrometers. The value of τ is dependent on the ratio of large to small aerosols, with large τ indicating the presence of high concentrations of small aerosols (e.g., smoke aerosols from biomass burning), and small τ indicating the presence of large aerosols, e.g., dust. Observational studies have made use of this size information such as small ($0.1 < r_e < 0.25 \mu\text{m}$) and coarse modes ($1.0 < r_e < 2.5 \mu\text{m}$) [sac1] AOT at 0.55 μm to discriminate between various aerosol types (e.g., [1]). The ratio of small to total AOT is known as the fine mode fraction (FMF) and has proven quite successful in separating predominately naturally occurring (coarse mode) from anthropogenic (small mode) aerosols [1], although it is a difficult parameter to validate [3]. In this method, MODIS AOT and FMF at 0.55 μm are used to separate the total AOT into various aerosol components using several thresholds [1]. AOT components are separated by first assuming that the maritime AOT is solely a linear function of near-surface wind speed over the ocean. The dust and anthropogenic components of the AOT are then solved using a mathematical relationship derived between the total AOT, the maritime AOT, the observed FMF, and the FMF thresholds. However, there are many assumptions required when separating the total AOT into various components such as the FMF thresholds themselves, and assuming that all small-mode aerosols are anthropogenic also leads to uncertainties in aerosol component radiative effects [3], [4].

The aerosol classification used by Kaufman *et al.* [1] and others generally uses aerosol information from only a single channel (usually at 0.55 μm), overlooking differences in the multispectral response for different aerosol types. Since each channel is highly correlated, we apply the principal component analysis (PCA) to extract the independent signals that are present in the seven-channel radiance data. Tanre *et al.* [5] used a similar PCA approach using theoretical radiance values for MODIS aerosol channels and observed that the AOT for small-mode aerosols decreases as a function of the wavelength much more quickly than for coarse-mode aerosols. Zubko *et al.* [6] extended this technique to other parameters, such as the single

Manuscript received November 27, 2007; revised February 23, 2008. This work was supported in part by the National Aeronautics and Space Administration (NASA) Radiation Sciences Program, in part by the NASA Interdisciplinary Sciences Program, in part by an Earth Observing System Grant, and in part by the Atmospheric Chemistry Modeling and Analysis Program.

The authors are with the Department of Atmospheric Science, The University of Alabama in Huntsville, Huntsville, AL 35805 USA (e-mail: tjones@nsstc.uah.edu; sundar@nsstc.uah.edu).

Color versions of one or more of the figures in this paper are available online at <http://ieeexplore.ieee.org>.

Digital Object Identifier 10.1109/TGRS.2008.920019

90 scattering albedo, the viewing angles, and the surface wind
 91 speed. Results from both efforts observed that two or three in-
 92 dependent pieces of information can be retrieved from MODIS
 93 multispectral radiance values through the PCA, and that these
 94 pieces of information account for more than 90% of the total
 95 variance present within the raw data. However, very little
 96 research has occurred that utilizes the multispectral characteris-
 97 tics of various aerosol species in aerosol classification using the
 98 PCA. In this study, the PCA is applied to the Terra MODIS
 99 radiance data at each channel, thereby producing a new set
 100 of independent channels, with each new channel sensitive to
 101 different aerosol characteristics. These data are then compared
 102 with the Goddard Global Ozone Chemistry Aerosol Radiation
 103 Transport (GOCART) modeled aerosol speciation during the
 104 same month and the Aerosol Robotic Network (AERONET)
 105 data from several sites that are known to have a single predom-
 106 inant aerosol species. The goal is to determine if multispectral
 107 PCA will provide information on aerosol species that cannot be
 108 observed using the $0.55\text{-}\mu\text{m}$ AOT and/or FMF alone.

109

II. DATA AND METHODS

110 Terra MODIS radiance values at $0.47, 0.55, 0.66, 0.86, 1.24,$
 111 1.64 , and $2.12\text{ }\mu\text{m}$ are obtained over the global oceans only
 112 from the MOD04, Collection 5 aerosol product [7], with a
 113 spatial resolution of 10 km^2 at nadir. We use the raw radiance
 114 values as inputs to the PCA rather than the retrieved AOT
 115 values at each wavelength since AOT retrievals are already a
 116 function of all seven radiance channels. For increasing aerosol
 117 concentrations, for scattering types of aerosols, larger amounts
 118 of short-wave radiation are scattered back to the satellite, re-
 119 sulting in a higher observed top of atmosphere radiance values.
 120 The AOT values over the ocean are retrieved from MODIS
 121 radiance values using a combination of four small-mode and
 122 five coarse-mode aerosol models with the relative amounts of
 123 small-mode to coarse-mode aerosols adjusted until a solution
 124 is found, which minimizes the error across the seven radiance
 125 values [2]. As a result, the reported AOT values at a certain
 126 wavelength are dependent on the radiance values from other
 127 channels. Using the retrieved AOT would induce uncertainties
 128 and biases that are present in the MODIS aerosol models into
 129 the research presented here. Thus, we chose to use the mea-
 130 sured MODIS cloud-free radiance values as inputs to the PCA
 131 rather than any derived products. MODIS data are collected for
 132 August 2004 due to the variety of differing aerosol types around
 133 the globe during this month. MODIS AOT and FMF from the
 134 MOD04 level 2 product from the Terra satellite along with the
 135 AERONET AOT values are used to help interpret the PCA
 136 components. The AERONET is a network of well-calibrated
 137 ground-based sun photometers that provide spectral AOT and
 138 other aerosol properties from hundreds of locations around
 139 the world [8]. We use the data for August 22, August 16,
 140 and August 10, 2004, from AERONET sites Capo Verde,
 141 Gosan (Korea), and Ascension Island, which are compared
 142 and colocated with the MODIS AOT data for that day. Data
 143 from these days were selected based on times when both good
 144 quality AERONET and MODIS data exist. For a particular
 145 day, MODIS AOT data within $\pm 1^\circ$ of the AERONET site

were averaged and compared to the AERONET observations. 146
 Each site location represents where the primary aerosol source 147
 (other than maritime sea salt) is known *a priori* from GOCART, 148
 including dust, fossil fuel combustion, and biomass burning, 149
 respectively. 150

The satellite-retrieved AOT and FMF are compared with the 151
 aerosol species simulations produced by the GOCART model 152
 [9]. GOCART simulates the transport of aerosols and their 153
 type over a global domain on a monthly averaged timescale. 154
 GOCART uses global emissions of aerosols and assimilated 155
 meteorological fields to separately calculate the mass loading 156
 of each aerosol species, which are then converted to the AOT 157
 using mass extinction coefficients. Aerosols are categorized as 158
 black carbon (BC), organic carbon (OC), sulfate (SU), dust 159
 (DU), and sea salt (SS). Organic carbon and sulfate are also 160
 split into anthropogenic and naturally occurring components, 161
 the latter generally from dimethyl sulfide (DMS). Monthly 162
 averaged data for August 2004 were acquired for an ocean only, 163
 global domain and were interpolated to a $2^\circ \times 2^\circ$ grid. 164

The statistical technique of the PCA enables the reduction 165
 of multiple and highly correlated data attributes into a fewer 166
 number of independent variables, each with a unique physical 167
 interpretation [10], [11]. The initial step in the PCA is the 168
 calculation of a correlation matrix between each of the input 169
 channels, which are the radiance values at all seven MODIS 170
 channels. Once the correlation matrix is computed, eigenvalues 171
 and vectors are calculated from the correlation matrix to deter- 172
 mine the weighting coefficients, which are then applied to the 173
 radiance data to produce the new independent pseudochannels 174
 (or PC channels). Each PC channel is ordered in such a way 175
 that the first channel (PC1) accounts for the greatest variance 176
 in the raw data, with the next (PC2) accounting for the next 177
 highest amount of variance, and so on. For this paper, the total 178
 number of pseudochannels created is equal to the number of 179
 input channels, which is seven. For illustration purposes, PC 180
 values are normalized to a $0\text{--}1.0$ scale and averaged to a $2^\circ \times 2^\circ$ 181
 resolution grid to correspond with the monthly averaged GO- 182
 CART data resolution. To visualize the sensitivity of the PC 183
 channels to aerosol properties, we compare GOCART and 184
 MODIS data as a function of the PC value. PC values are binned 185
 at 0.05 intervals, and, for each bin, the ratio of the GOCART 186
 component AOT to the total AOT is calculated for grid cells 187
 within a particular PC bin. To compare the effectiveness of the 188
 PC classification with the $0.55\text{-}\mu\text{m}$ FMF classification, a similar 189
 procedure is used but using a 0.05 FMF interval bin. 190

III. RESULTS

A. PC Weightings

As expected, solar radiance from each of the seven MODIS 193
 aerosol channels is highly correlated, although the correlation 194
 does decrease to < 0.5 when comparing $0.47\text{-}2.13\text{-}\mu\text{m}$ 195
 radiance values. Analysis of the eigenvalues associated with 196
 each PC channel indicates that 78.4% of the variance is ex- 197
 plained by PC1, 19.7% by PC2, and 1.4% by PC3, with PC1– 198
 PC3 accounting for $\sim 99\%$ of the total variance, similar to that 199
 expected in [5] and [6]. The amount explained by PC4–PC7 200
 combined is less than 1%, with no consistent patterns observed 201

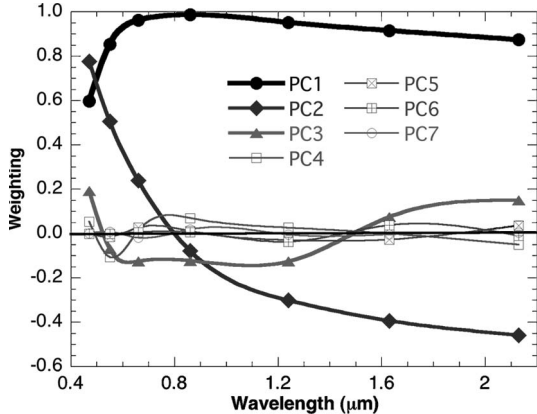


Fig. 1. Weighting coefficients derived from the PCA for PC channels 1–7. Magnitudes indicate the relative importance of each original channel to the resulting PC channel. Note that weightings for PC4–PC7 are very small compared to those for PC1–PC3.

202 in the weighting coefficients. Thus, we are confident that nearly
203 all of the physical signals present in the seven-channel radiance
204 data are taken into account by the first three pseudochannels
205 (PC1–PC3). These values are only representative of the one-
206 month data set examined here; however, they remain rel-
207 atively constant compared to the remaining 11 months of
208 2004: $74\% < \text{PC1} < 84\%$; $15\% < \text{PC2} < 24\%$; $1\% < \text{PC3} <$
209 2%. The physical interpretation of PC1–PC3 also remains the
210 same despite the presence of differing aerosol concentrations
211 and types from month to month.

212 Raw weighting coefficients as a function of the MODIS
213 wavelength are plotted in Fig. 1. The coefficients indicate
214 the relative contribution of each original channel to the new
215 pseudochannel. PC1 has, by far, the highest weightings com-
216 pared to PC2 and PC3. Physically, PC1 represents a weighted
217 mean or “multispectral” radiance value that is directly propor-
218 tional to the aerosol concentration, with low values of PC1
219 corresponding to low values of the AOT (for all original wave-
220 lengths), whereas high PC1 values correspond to high values
221 of the AOT at $0.55\text{ }\mu\text{m}$ (Fig. 2). The correlation between PC1
222 and the AOT at $0.55\text{ }\mu\text{m}$ is high ($r = 0.89$) and is generally
223 linear for $\text{AOT} < 1.0$. This linear relationship is similar to that
224 observed between the AOT and the broadband short-wave flux,
225 which itself is highly correlated with the MODIS narrow-band
226 short-wave observations [12].

227 A more interesting relationship exists in PC2. Weighting
228 coefficients for PC2 decrease as the MODIS wavelength in-
229 creases, and range from 0.78 at $0.47\text{ }\mu\text{m}$ (blue) to -0.46 at
230 $2.12\text{ }\mu\text{m}$ (near infrared) with a weighting of near zero at
231 $0.86\text{ }\mu\text{m}$ (Fig. 1). Due to its small weighting coefficient, the
232 radiance at $0.86\text{ }\mu\text{m}$ contributes very little to PC2 values.
233 These weightings indicate that PC2 is the most sensitive to
234 the difference between blue and red radiance values, which
235 would be greatest for aerosols that scatter more radiation in
236 the blue portion of the spectrum and for aerosols that scatter
237 proportionally less radiation in the near-infrared portion of the
238 spectrum. Compared to PC1, PC2 is only weakly correlated
239 with the AOT at $0.55\text{ }\mu\text{m}$, with a correlation coefficient of
240 only -0.11 (Fig. 2). However, the correlation between PC2 and
241 the FMF at $0.55\text{ }\mu\text{m}$ is much higher, i.e., 0.54, indicating the

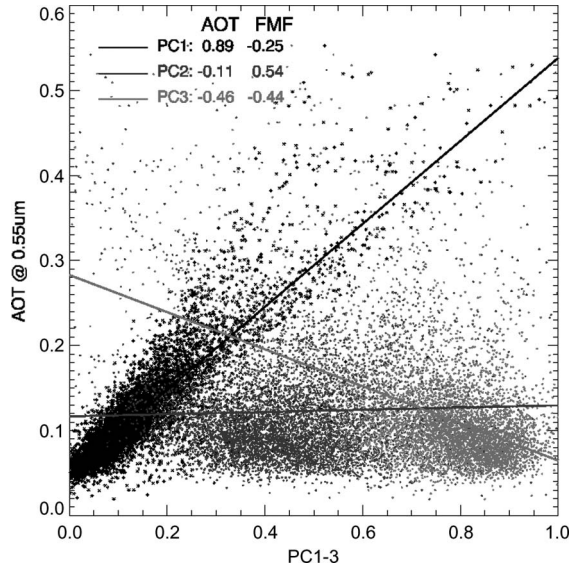


Fig. 2. Scatterplot of monthly averaged MODIS AOT at $0.55\text{ }\mu\text{m}$ as a function of normalized PC1, PC2, and PC3 values. Best-fit lines along with linear correlation coefficients between PC values and MODIS AOT and FMF are also given.

dependence on the aerosol size. A similar result was observed 242 by Tanre *et al.* [5], who also noted that this relationship was 243 the most important for small-sized aerosols ($r_e < 0.3\text{ }\mu\text{m}$). 244 Previous research has observed that anthropogenic aerosols, 245 which are primarily small mode in nature, often have higher 246 blue versus near-infrared radiance values (e.g., [13]). Thus, 247 PC2 could be useful for separating naturally occurring from 248 anthropogenic aerosol regions since it is correlated with aerosol 249 size properties. 250

The interpretation of PC3 is not as clear as those of PC1 and 251 PC2. Weighting coefficient values are quite small ($< \pm 0.2$) and 252 are positive for MODIS $0.47\text{-, }1.24\text{-, and }2.12\text{-}\mu\text{m}$ channels, 253 but negative for the remaining four channels. PC3 shows a 254 modest inverse correlation with the AOT and the FMF at 255 $0.55\text{ }\mu\text{m}$ ($r = -0.46, -0.44$; Fig. 2). Interestingly, the shape 256 of the weighting coefficient curve mirrors that observed for 257 PC1 to some extent, which is consistent with the reversed sign 258 of the AOT correlation. Although PC3 only explains a small 259 proportion of the total variance, the significance of the AOT 260 and FMF correlations suggests that it is indeed an actual signal 261 and not random noise. The correlation between PC4–PC7 and 262 the AOT or the FMF at $0.55\text{ }\mu\text{m}$ never exceeds 0.15, making 263 the physical interpretation of these channels difficult if such an 264 interpretation exists at all. 265

Additional evidence for the physical interpretation of PC 266 channels can be found when comparing multispectral MODIS 267 and AERONET AOT values for locations where the predomi- 268 nant aerosol source is known. The locations selected are Capo 269 Verde, Gosan (Korea), and Ascension Island, whose aerosol 270 concentrations are largely from dust, fossil fuel combustion, 271 and biomass burning, respectively. Fig. 3 shows MODIS and 272 AERONET AOT values as a function of the wavelength. For 273 all three locations, MODIS AOT decreases as a function of the 274 wavelength. However, the decrease is much more significant 275 (compared to the average AOT across all channels) for Gosan 276

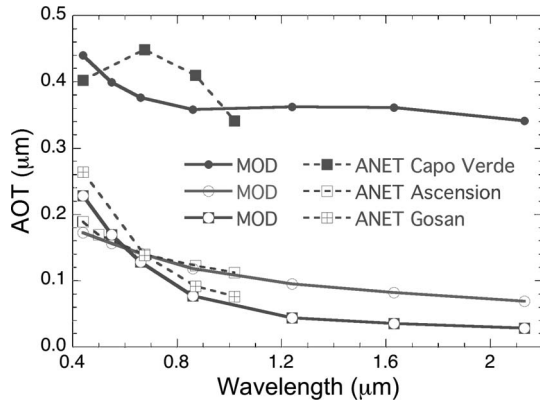


Fig. 3. MODIS (MOD) and AERONET (ANET) AOT between 0.4 and 2.2 μm for three sites, Capo Verde, Gosan (Korea), and Ascension Island, each representing significant dust, industrial pollution, and biomass burning aerosol concentrations, respectively. Note the similarities between Gosan and Ascension Island AOT and PC2 weighting coefficients.

277 (Korea) and Ascension Island locations, where small-mode
278 aerosol concentrations are significant [14]. AERONET AOT for
279 these two sites closely follows that of MODIS AOT, although
280 some differences were observed at Capo Verde. Levy *et al.* [15]
281 noted the differences in the multispectral response to dust
282 aerosols between MODIS and AERONET measurements. Their
283 differences are different than those observed here; however,
284 we use Collection 5 data, which have improved coarse-mode
285 aerosol models not used by Levy *et al.* [15]. However, the
286 spectral response for small-mode aerosols for both MODIS
287 and AERONET AOT remains clearly significant. Also, the de-
288 creasing AOT as a function of increasing wavelength for these
289 aerosols corresponds quite well with the weighting coefficients
290 for PC2, indicating that it is indeed sensitive to the aerosol size
291 (Figs. 1 and 3).

292 The usefulness of this multispectral approach toward aerosol
293 classification is evident when creating a three-band overlay
294 using normalized PC1, PC2, and PC3 values (Fig. 4). Here,
295 high values of PC1, PC2, and PC3 are denoted by red, green,
296 and blue colors, respectively. Brightness increases as the values
297 for PC1–PC3 become larger. It is immediately clear that aerosol
298 speciation information is evident when utilizing the first three
299 PC channels. Regions normally associated with dust (eastern
300 North Atlantic and western Arabian Sea) in August appear
301 as pink and red, which indicates that high values of PC1
302 correspond to high concentrations of dust aerosols compared
303 to other aerosol types. Yellow-green regions are present in the
304 South Atlantic Ocean off west of Africa and, to a lesser degree,
305 in Indonesia and east of China. Anthropogenic aerosols, in
306 the form of sulfates and organic carbon, are the predominant
307 aerosol types in these regions. The signal is most evident in the
308 South Atlantic, where large amounts of aerosols from biomass
309 burning are transported over the ocean. Since the AOT is high
310 and the FMF is low, PC1 and PC2 values are high, resulting
311 in the yellow color observed. Light blues and greens are also
312 evident off the east coasts of the U.S. and northern Europe.
313 Compared to the dust and biomass burning regions, the total
314 AOT is low (low red values), but the anthropogenic (particularly
315 sulfate) proportion of aerosols is high resulting in the greenish
316 appearance. Regions over the open oceans appear blue, corre-

sponding to high values of PC3. Here, aerosol concentrations 317 are generally low (low PC1) and consist of maritime sea salt 318 and DMS (low PC2). In the Southern Hemisphere south of 319 35 °S, somewhat higher values of PC1 were observed, possibly 320 resulting from larger sea-salt concentrations due to high wind 321 speeds or cloud contamination [16].

B. PC Values Compared to GOCART Aerosol Components

To determine the sensitivity of each PC channel to specific 324 aerosol properties, PC1–PC3 values are compared to monthly 325 averaged GOCART model-generated aerosol speciation over 326 the global oceans for August 2004. Fig. 5(a)–(c) shows av- 327 erage MODIS AOT and FMF at 0.55 μm as a function of 328 normalized PC1–PC3, binned at 0.05 intervals. Also plotted 329 is the percentage of the total GOCART AOT at 0.55 μm 330 accounted for by one of the six aerosol species, including 331 sea salt (SS), dust (DU), black carbon (BC), anthropogenic 332 organic carbon (OC), anthropogenic sulfate (SU), and naturally 333 occurring sulfate (NSU). MODIS AOT increases from 0.08 to 334 0.60 as PC1 increases from 0 to 1.0, as should be the case given 335 the high correlation between PC1 and short-wave radiance at 336 most channels [Fig. 5(a)]. The FMF remains roughly constant 337 at ~ 0.5 when $0.2 < \text{PC1} < 0.8$, although it does vary at the low 338 and high extremes of PC1. Comparing PC1 values to GOCART 339 aerosol speciation shows several interesting features. The nat- 340 urally occurring portion of organic carbon was always small, 341 never being greater than 3%, and, thus, was not plotted. DMS 342 accounts for up to 15% when $\text{PC1} < 0.2$, but less than 10% 343 thereafter. The anthropogenic sulfate concentration remains 344 between 20% and 25% for all PC1 bins. However, the dust 345 aerosol concentration does substantially change as a function of 346 PC1, ranging from 15% to 50% at the expense of sea salt and 347 natural and organic sulfate concentrations. Since low aerosol 348 concentrations often occur over the open oceans, the high sea- 349 salt concentration at low PC1 values should exist, although, 350 even for low PC1 values, the total sea-salt portion of the AOT 351 does not exceed 30%. The low values of PC1 ($\text{PC} < 0.2$) 352 correspond to relatively pristine ocean conditions, where sea 353 salt and DMS are the primary aerosol species, whereas the high 354 values of PC1 correspond to high dust aerosol concentrations. 355 PC1 values show little sensitivity to black and organic carbon 356 concentrations.

Aerosol properties also substantially change as a function of 358 PC2 values [Fig. 5(b)]. Unlike PC1, PC2 is sensitive to changes 359 in the aerosol size, evidenced by the increasing FMF values 360 as a function of PC2. Moreover, unlike PC1, PC2 is not very 361 sensitive to the total aerosol concentration with a very little 362 change in MODIS AOT when $0.2 < \text{PC2} < 0.8$, whereas the 363 FMF increases from 0.3 to 0.7 over that same range. Corre- 364 sponding to this increase in the FMF, anthropogenic organic 365 carbon and sulfate, which are both generally considered small- 366 mode aerosols, substantially increase accounting for over 50% 367 of the total AOT when $\text{PC2} > 0.8$. The portion of the AOT 368 due to black carbon also slightly increases, but remains below 369 10%. The dust aerosol concentration generally represents less 370 than 20% of the total AOT for all PC2 bins, with no apparent 371 trends. The sea-salt concentration rapidly decreases with values 372

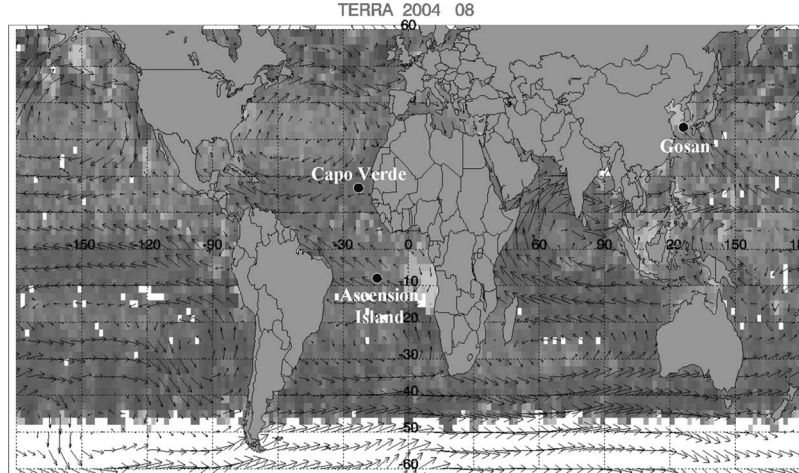


Fig. 4. Three-band overlay of normalized (red) PC1, (green) PC2, and (blue) PC3 values for August 2004. Locations of AERONET sites (Capo Verde, Gosan, and Ascension Island) are represented by black circles.

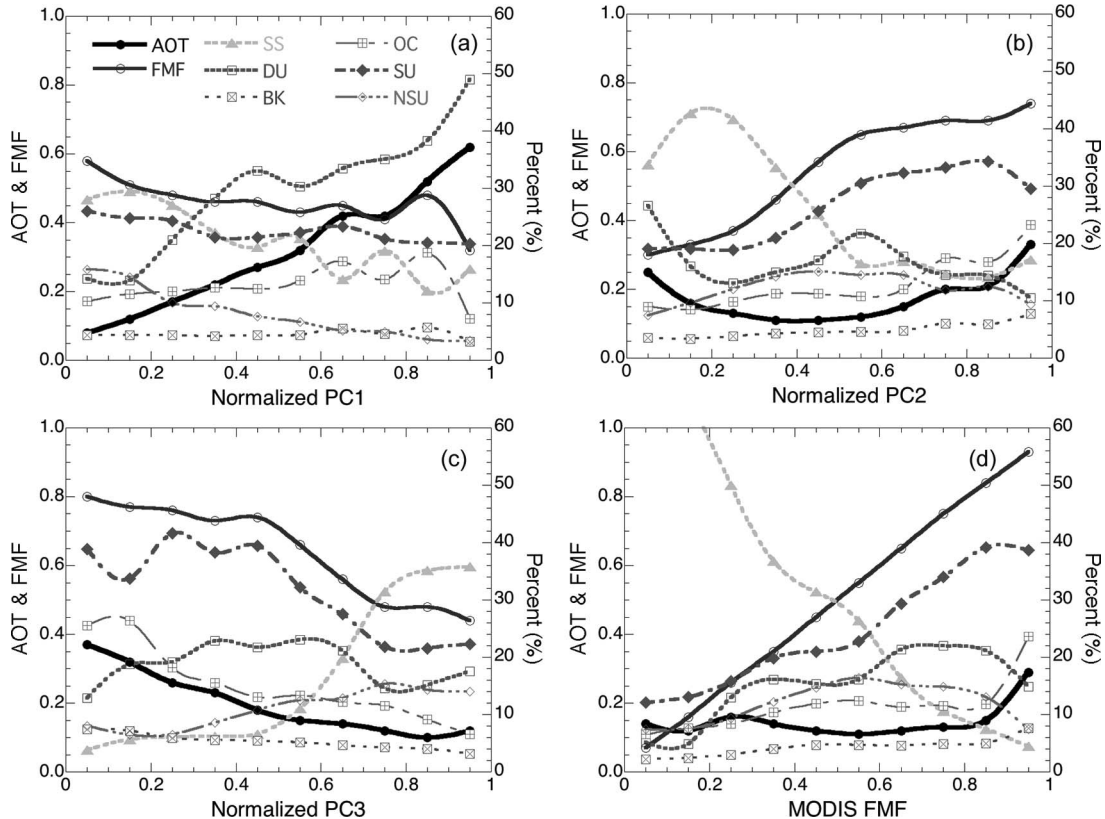


Fig. 5. MODIS AOT, FMF, and GOCART-modeled contribution to the total AOT for six major aerosol species (sea salt, dust, black carbon, anthropogenic organic carbon, anthropogenic sulfate, and naturally occurring sulfate) as a function of a normalized PC value for (a) PC1, (b) PC2, (c) PC3, and (d) FMF at $0.55 \mu\text{m}$.

373 exceeding 40% for $\text{PC2} < 0.3$, but decreasing to less than 20%
 374 thereafter. These results indicate that PC2 are the sensitive
 375 aerosols produced from anthropogenic sources, particularly
 376 biomass burning occurring off the African coast (Fig. 4). For
 377 PC2 greater than 0.8, the total anthropogenic component of the
 378 AOT ($\text{BC} + \text{OC} + \text{SU}$) represents over 60% of the total AOT
 379 modeled by GOCART, whereas the combined dust and sea-salt
 380 contribution represents less than 30% of the total AOT.
 381 The third PC channel, i.e., PC3, is an interesting case.
 382 Although it only accounts for 1.4% of the total variance,

the weighting coefficients show a distinct pattern, somewhat 383 mirroring the shape of PC1 weightings (Fig. 1). Fig. 2 suggests 384 that PC3 is equally sensitive to the aerosol concentration as well 385 as the aerosol size parameters. Comparing PC3 values against 386 GOCART-modeled aerosol species also reveals that this PC is 387 also useful in the separation of aerosol species. Unlike PC1 388 and PC2, sea-salt and DMS contributions increase for larger 389 PC3 values that when combined, become $> 50\%$ for $\text{PC3} > 0.8$ [Fig. 5(c)]. A corresponding decrease in anthropogenic 391 organic carbon and sulfate is also observed, with little overall 392

393 sensitivity to the dust aerosol concentration. The decrease in
 394 anthropogenic aerosol concentrations corresponds with similar
 395 decreases in MODIS FMF and AOT values [Figs. 2 and 5(c)].
 396 Thus, PC3 can be said to be inversely proportional to the aerosol
 397 size and the total aerosol concentration, PC1 is primarily sen-
 398 sitive to the total aerosol concentration, and PC2 is primarily
 399 sensitive to the aerosol size but not to the concentration, consis-
 400 tent with Fig. 2. PC3 is statistically independent to PC2; thus,
 401 the multispectral radiance values are providing two independent
 402 sources of aerosol size and concentration information.

403 The exact physical mechanism behind PC3 remains unclear;
 404 however, spatial plots of PC3 alone (not shown) clearly show
 405 high values in maritime regions, whereas the plots show very
 406 low values in regions associated with aerosols transported
 407 from biomass burning sources. One possible hypothesis is the
 408 sensitivity of the 0.47- μm channels toward ocean reflectance,
 409 which also happens to have a positive weighting coefficient in
 410 PC3 (Fig. 1). Thus, it is possible that the high values of PC3
 411 correspond to low AOT concentrations when the ocean re-
 412 flectance signal is the strongest. Similarly, PC3 is minimized
 413 when the AOT is high, masking the ocean reflectance signal
 414 from the satellite. However, this hypothesis still does not ex-
 415 plain the positive coefficients present at 1.63- and 2.12- μm
 416 wavelengths. This remains a question for future research to
 417 answer. For higher order PC channels (PC4–PC7), there ap-
 418 pears to be very little sensitivity to aerosol properties. With the
 419 exception of weak sensitivity to the natural sulfate concentra-
 420 tion for PC5, GOCART-modeled aerosol properties showed no
 421 consistent trends as a function of PC values (not shown). For the
 422 purposes of aerosol classification, these channels provide little
 423 in the way of useful information.

424 C. MODIS FMF Values Compared to GOCART 425 Aerosol Components

426 To determine if principal components are indeed useful, we
 427 perform the same analysis as above, but for MODIS FMF
 428 values [Fig. 5(d)]. It is quite evident that FMF values are an
 429 excellent way to distinguish among sea-salt and anthropogenic
 430 sulfate and organic carbon aerosols. When $\text{FMF} < 0.2$, the
 431 proportion of the AOT from sea salt exceeds 60%, whereas
 432 the anthropogenic aerosol contribution approaches 60% for
 433 $\text{FMF} > 0.8$, with most of the anthropogenic contribution being
 434 from sulfate. However, the FMF alone is not very sensitive
 435 to the dust aerosol concentration. There is an increase in the
 436 dust proportion from $\sim 10\%$ at a low FMF to $\sim 20\%$ at a high
 437 FMF, which actually contradicts the expectations. Generally,
 438 dust aerosols have larger particle sizes than the anthropogenic
 439 components: thus, one would expect the dust concentrations to
 440 be greatest somewhere around $\text{FMF} \approx 0.5$ [1]. At least for the
 441 time period used here, dust aerosols are sufficiently mixed with
 442 other aerosol types for their signal to be not apparent in MODIS
 443 FMF observations alone. However, performing the PCA on
 444 the raw MODIS radiance values produces a pseudochannel
 445 (PC1) that is sensitive to the dust aerosol concentration to
 446 a much higher degree. Since PC1 is highly correlated with
 447 the total AOT, one might expect that the total AOT is also
 448 sensitive to the dust aerosol concentration; however, this, again,

449 was not observed here (not shown). Rather, we believe that
 450 it is the multispectral response of dust aerosols compared to
 451 anthropogenic types that produces this signal. These differences
 452 are apparent in Fig. 1, with the AERONET AOT dust spectral
 453 dependence being of different shape than the other two aerosol
 454 types. This shape is quite similar to the weighting value curve
 455 plotted in Fig. 1; thus, high concentrations of dust are most
 456 likely to result in high values of PC1. 456

D. Application of Weighting to Independent Data

457

To access the applicability of the weighting coefficients to 458 independent data, we apply the coefficients derived from the 459 Terra data above to the MODIS data from the Aqua satellite 460 acquired for the same month (August 2004). Aside from the 461 Aqua overpass being 3–4 h after Terra, everything else related 462 to the retrievals of aerosol radiance should be the same. If we 463 assume that aerosol properties do not significantly change in 464 this short time, applying the Terra weighting coefficients to 465 Aqua data should produce good results. The Terra weighting 466 coefficients are applied to the Aqua MODIS radiance values 467 producing one set of PC data, which are compared with another 468 set of PC data produced from the Aqua radiance values using 469 the weighing coefficients derived from the Aqua data itself. The 470 resulting correlation between these data is greater than 0.99 471 for PC1–PC3. For higher order PC channels, the correlation 472 substantially decreases, as random noise becomes a more sig- 473 nificant factor. 474

IV. CONCLUSION

475

We have shown that multispectral AOT data from the MODIS 476 satellite in conjunction with GOCART can be used to extract 477 important aerosol type information without the use of small- 478 mode AOT values. The PCA condenses seven highly correlated 479 radiance channels into a smaller number of independent PC 480 channels, each with its own physical interpretation. Using the 481 monthly averaged GOCART data as a guide, it becomes appar- 482 ent that different PC channels are sensitive to various aerosol 483 species and mixtures thereof. We show that PC1 and PC3 can 484 distinguish between pristine (sea salt and DMS) and heavy 485 dust aerosol concentrations, whereas PC2 is very sensitive to 486 anthropogenic aerosol concentrations, with high PC2 values 487 corresponding to a 60% or greater anthropogenic component 488 to the total AOT. PC data, particularly PC1, are much more 489 sensitive to the dust aerosol concentration compared to the use 490 of simple FMF thresholds. Since dust aerosol concentrations 491 are often the most difficult type to extract on an objective basis, 492 perhaps future works could take advantage of the approach 493 examined here. It is likely that the use of higher spatial and tem- 494 poral resolution aerosol speciation modeling allows for even 495 better multispectral aerosol characteristics to be drawn. With 496 higher resolution GOCART data, higher order PC channels may 497 also be able to provide additional information into the observed 498 aerosol properties. Given the problems noted with satellite- 499 derived aerosol parameters over land, the use of multispectral 500 information provides another, possibly more effective, avenue 501 for aerosol classification over land. Future research will analyze 502

503 this possibility using larger data sets encompassing multiple
504 years of observations.

505

ACKNOWLEDGMENT

506 The Clouds and the Earth's Radiant Energy System (CERES)
507 Single Scanner Footprint data, which contain the merged
508 MODIS and CERES and the Measurements of Pollution in
509 the Troposphere data were obtained through the NASA Lan-
510 gley Distributed Active Archive Systems. The MODIS daily
511 products were obtained from the Goddard Distributed Active
512 Archive Systems. The authors would like to thank Dr. M. Chin
513 for providing the GOCART results.

514

REFERENCES

- 515 [1] Y. J. Kaufman, O. Boucher, D. Tanre, M. Chin, L. A. Remer,
516 and T. Takemura, "Aerosol anthropogenic component estimated from
517 satellite data," *Geophys. Res. Lett.*, vol. 32, no. 17, L17 804, 2005.
518 DOI:10.1029/2005GL023125.
- 519 [2] L. A. Remer, Y. J. Kaufman, D. Tanré, S. Mattoo, D. A. Chu,
520 J. V. Martins, R.-R. Li, C. Ichoku, R. C. Levy, R. G. Kleidman, T. F. Eck,
521 E. Vermote, and B. N. Holben, "The MODIS aerosol algorithm, products,
522 and validation," *J. Atmos. Sci.*, vol. 62, no. 4, pp. 947–973, Apr. 2005.
- 523 [3] T. L. Anderson *et al.*, "An 'A-Train' strategy for quantifying direct climate
524 forcing by anthropogenic aerosols," *Bull. Amer. Meteorol. Soc.*, vol. 86,
525 no. 12, pp. 1795–1809, Dec. 2005.
- 526 [4] T. A. Jones and S. A. Christopher, "Statistical variability of top of at-
527 mosphere cloud-free shortwave aerosol radiative effect," *Atmos. Chem.
528 Phys. Discuss.*, vol. 7, pp. 2937–2948, 2007.
- 529 [5] D. Tanre, M. Herman, and Y. J. Kaufman, "Information on aerosol size
530 distribution contained in solar reflected spectral radiances," *J. Geophys.
531 Res.*, vol. 101, no. D14, pp. 19 043–19 060, 1996.
- 532 [6] V. Zubko, Y. J. Kaufman, R. I. Burg, and J. V. Martins, "Principal com-
533 ponent analysis of remote sensing of aerosols over oceans," *IEEE Trans.
534 Geosci. Remote Sens.*, vol. 45, no. 3, pp. 730–745, Mar. 2007.
- 535 [7] L. A. Remer, D. Tanre, and Y. Kaufman, *Algorithm for Remote Sensing of
536 Tropospheric Aerosol From MODIS: Collection 5*, 2006.
- 537 [8] B. N. Holben *et al.*, "AERONET—A federated instrument network and
538 data archive for aerosol characterization," *Remote Sens. Environ.*, vol. 66,
539 no. 1, pp. 1–16, Oct. 1998.
- 540 [9] M. Chin *et al.*, "Aerosol distributions and radiative properties simulated in
541 the GOCART model and comparisons with observations," *J. Atmos. Sci.*,
542 vol. 59, pp. 461–483, 2002.
- 543 [10] T. A. Jones, K. M. McGrath, and J. T. Snow, "Association between
544 NSSL mesocyclone detection algorithm-detected vortices and tornadoes,"
545 *Weather Forecast.*, vol. 19, no. 5, pp. 872–890, Oct. 2004.
- 546 [11] D. S. Wilks, *Statistical Methods in the Atmospheric Sciences*. San Diego,
547 CA: Academic, 2006.
- 548 [12] N. G. Loeb and N. Manalo-Smith, "Top-of-atmosphere direct radiative
549 effect of aerosols over global oceans from merged CERES and MODIS
550 observations," *J. Climate*, vol. 18, no. 17, pp. 3506–3526, Sep. 2005.

- [13] T. F. Eck *et al.*, "Wavelength dependence of the optical depth of biomass
551 burning, urban, and desert dust aerosols," *J. Geophys. Res.*, vol. 104, 552
no. D24, pp. 31 333–31 349, 1999.
553
- [14] A. Smirnov, B. N. Holben, Y. J. Kaufman, O. Dubovik, T. F. Eck,
554 I. Slutsker, C. Pietras, and R. N. Halthore, "Optical properties of at-
555 mospheric aerosol in maritime environments," *J. Atmos. Sci.*, vol. 59, 556
no. 3, pp. 501–523, Feb. 2002.
557
- [15] R. C. Levy, L. A. Remer, S. Mattoo, E. F. Vermote, and Y. J. Kaufman,
558 "Second-generation operational algorithm: Retrieval of aerosol properties
559 over land from inversion of moderate resolution imaging spectroradiome-
560 ter spectral reflectance," *J. Geophys. Res.*, vol. 112, no. D13, D13 211, 561
Jul. 2007. DOI: 10.1029/2006JD007811.
562
- [16] J. Zhang, J. S. Reid, and B. N. Holben, "An analysis of potential
563 cloud artifacts in MODIS over ocean aerosol optical thickness prod-
564 ucts," *Geophys. Res. Lett.*, vol. 32, no. 15, L15 803, Aug. 2005. DOI:
565 10.1029/2005GL023254.
566



Thomas A. Jones received the B.S. and M.S. 567 degrees in meteorology from the University of 568 Oklahoma, Norman, in 2000 and 2002, respectively, 569 while focusing on the development of regional thun- 570 derstorm climatologies, and the Ph.D. degree from 571 The University of Alabama in Huntsville, Huntsville, 572 in 2006 while specializing in improving hurricane in- 573 tensity change forecasts using satellite-derived pas- 574 sive microwave imagery. 575

Since May 2006, he has been a Research Scientist 576 with The University of Alabama in Huntsville. He 577 has a wide range of research interests within the atmospheric sciences commu- 578 nity. He is currently researching the effect of aerosols, and their subspecies, on 579 short-wave and long-wave radiative effects using MODIS and CERES data. He 580 is extending this research to include the effects of meteorological conditions on 581 aerosols and the aerosol's effect to clouds. 582



Sundar A. Christopher received the M.S. degree 583 in meteorology from the South Dakota School of 584 Mines and Technology, Rapid City, in 1989, the M.S. 585 degree in industrial/organizational psychology from 586 The University of Alabama in Huntsville (UAH), 587 Huntsville, in 2002, and the Ph.D. degree in at- 588 mospheric sciences from the Colorado State Univer- 589 sity, Fort Collins, in 1995. 590

He is currently a Professor with the Department of 591 Atmospheric Sciences and the Associate Director of 592 the Earth System Science Center, both at UAH. His 593 research interests include satellite remote sensing of clouds and aerosols and 594 their impact on air quality and global and regional climate. 595